Journal of the Chinese Institute of Engineers
Publication details, including instructions for authors and subscription information:
http://www.tandfonline.com/loi/tcie20

Genetic fuzzy logic traffic signal control with cell transmission modeling

Yu-Chiun Chiou[a] & Yen-Fei Huang[a]
[a] Institute of Traffic and Transportation, National Chiao Tung University, Taipei, Taiwan.
Published online: 25 Jul 2013.

Journal of the Chinese Institute of Engineers, 2014
Vol. 37, No. 4, 446–460, http://dx.doi.org/10.1080/02533839.2013.814995

Genetic fuzzy logic traffic signal control with cell transmission modeling

Yu-Chiun Chiou* and Yen-Fei Huang

Institute of Traffic and Transportation, National Chiao Tung University, Taipei, Taiwan

(*Received 19 August 2011; final version received 2 October 2012*)

This study develops an adaptive traffic signal control model based on an iterative genetic fuzzy logic controller (GFLC). The proposed model considers traffic flow and queue length as state variables and extension of green time as control variable, toward the minimization of total vehicle delays. For the learning efficiency of GFLC and the capability in capturing traffic behaviors, cell transmission model is used to replicate the traffic condition. To investigate, the performance of the proposed model in the case of an isolated intersection, comparisons to pretimed signal timing plans determining by Webster and total enumeration methods, and two queue-length based adaptive models are conducted. Results show that our proposed GFLC model performs best. As traffic flows vary more noticeably, the GFLC traffic signal control model performs even better than any timing plans. In the case of sequential intersections with four coordinated signal systems: simultaneous, progressive, alternate, and independent, the experimental example study also show that the proposed GFLC model can also perform better than current and pretimed timing plans, suggesting that the proposed GFLC signal control model is effective, robust, and adaptable.

Keywords: adaptive signal control; genetic fuzzy logic controller; cell transmission model

1. Introduction

On-line traffic signal control typically feeds real-time traffic data, collected by sensors, into a build-in controller to produce timing plans. Thus, it can provide signal-timing plans in response to real-time traffic conditions. Actuated signal control, dynamic signal control, and adaptive signal control are examples of on-line control. Because of its flexibility, adaptability, and optimality, adaptive signal control tends to be the mainstream of signal controls nowadays. The well-known adaptive signal controllers, such as SCOOT, SCATS, and OPAC, employ mathematical equations or models to determine 'crisp' threshold values as the cores of control mechanisms; thus, the control performance may be negatively affected by the uncertainty of traffic conditions. Since a fuzzy control system has excellent performance in data mapping as well as in treating ambiguous or vague judgment (Teodorovic 1999), many recent studies have employed fuzzy set theory to develop fuzzy logic controllers (FLC). The underlying theory for an FLC system is to use fuzzy logic rules to form a control mechanism to approximate expert perception or judgment under given conditions (Zadeh 1973). The applications of FLC to signal control are to determine the signal phasing and timing plans, including priority of phases, cycle length and split, by utilizing real-time traffic data, such as vehicle arrivals or arrival rate, occupancy, queue length and speed, collected by detectors.

Most FLC signal control models consider some traffic variables as state variables, such as vehicle arrivals, queue length, occupancy, and green elapsed time and use of extension of green time as a control variable (Pappis and Mamdani 1977; Mohamed, Mohamed, and Murali 1999; Niittymäki 2001). Some studies further determine the phase sequence and green times of each phase (Hoyer and Jumar 1994; Murat and Gedizlioglu 2005). However, most of these studies subjectively preset the combination of logic rules and shapes of membership functions, lacking a learning procedure. Thus, the performance of the models cannot be assured. Adjusting the combination of logic rules and membership functions very often requires tremendous effort, but there is no guarantee of obtaining good control performance. Genetic algorithms (GAs) have been proven suitable for solving both combinatory optimization problem (e.g. selecting the logic rules) and parameter optimization problem (e.g. tuning the membership functions). Employing GAs to construct an FLC system with a learning process from examples, hereafter termed a genetic fuzzy logic controller (GFLC), cannot only avoid the bias caused by subjective settings of logic rules or membership functions but also greatly enhance the control performance. Thus, a considerable number of studies relating to different areas of GFLC have been published in recent years (Herrera, Lozano, and

*Corresponding author. Email: ycchiou@mail.nctu.edu.tw

Verdegay 1995, 1998; Lekova et al. 1998; Wang and Yen 1999; Chiou and Lan 2005). The iterative GFLC model proposed and validated by Chiou and Lan (2005) is adopted in this study.

However, to develop a GFLC-based signal control requires an efficient traffic simulation model to replicate traffic behaviors and determine the performance of the control logic. Many studies use microscopic traffic simulation software to evaluate the performances of signal control models, such as CORSIM (Pham et al. 2011), SimTraffic (Lin, Tung, and Ku 2010), AIMSUN (Fang and Elefteriadou 2010), VISSIM (Xu and Zheng 2009), MITSIMLab (Ben-Akiva et al. 2003), INTEGRATION (Dion, Rakha, and Zhang 2004), and PARAMICS (Wu and Ho 2009); however, it would be too time-consuming to use such simulation software for the evolution of genetic generations. Thus, this study employs a cell transmission model (CTM), a cell-based model proposed by Daganzo (1994, 1995), to evaluate the performance of learned logic rules and tuned membership function. CTM is a first-order discrete Godunov approximation to the kinematic wave partial differential equation of Lighthill and Whitham (1955) and Richards (1956). The popularity of CTM is due to its very low computation requirements compared with micro-simulation models; the ease with which it can be calibrated using routinely available point detector data (Munoz et al. 2004); its extensibility to networks (Waller and Ziliaskopoulos 2001) and urban roads with signalized intersections (Lo 2001; Wong, Wong, and Lo 2010); and the flexibility with which it can be used to pose questions of traffic assignment (Lo and Szeto 2002) and ramp metering (Zhang, Ritchie, and Recker 1996) and freeway speed-limit control (Chiou, Huang, and Lin 2010). Despite their simplicity, field data have suggested that they fit measurements well. See for example, Lin and Ahanotu (1995) and Smilowitz and Daganzo (1999). These two studies validated CTM for freeway and arterial traffic. According to the description above, CTM is a widely used discrete macroscopic model and can simulate, as well, plausible models for signalized urban streets.

Based on this, this study aims to develop an adaptive signal control model for both isolated and sequential intersections based on the iterative GFLC with a cell transmission modeling approach. The study is organized as follows. Section 2 states the rationales for signal control with an iterative GFLC model and CTM. Section 3 utilizes experimental cases to validate the effectiveness, robustness, and applicability of the proposed iterative GFLC model in controlling the signal at isolated intersections. Section 4 further validates the effectiveness and applicability of the iterative GFLC model in controlling the signal of sequential intersections. Finally, the concluding remarks and suggestions for future research follow.

2. Methods

2.1. *The GFLC model*

To develop a self-learning GFLC-based signal control model, the iterative GFLC model, proposed by Chiou and Lan (2005), is adopted in this study. The encoding methods, genetic operators, and iterative evolution algorithm for the iterative GFLC model are briefly described as follows.

2.1.1. *Encoding method for logic rules*

Each logic rule is represented by one gene and its linguistic degree of control variable is indicated by the value of the corresponding gene. Taking two state variables and one control variable as an example, if each variable has five linguistic degrees (*NL*: negative large, *NS*: negative small, *ZE*: zero, *PS*: positive small, *PL*: positive large), then the chromosome length is 25. Genes take the integers from zero to five, where zero represents the exclusion of the rules; other numbers indicate the inclusion of the rules and the linguistic degrees of control variable. This encoding method is depicted in Figure 1. A chromosome with gene sequence of 00020400100000010000030000, for example, will represent five logic rules being selected:

Rule 1: IF $x_1 = NL$ and $x_2 = PS$ THEN $y = NS$
Rule 2: IF $x_1 = NS$ and $x_2 = NL$ THEN $y = PS$
Rule 3: IF $x_1 = NS$ and $x_2 = PS$ THEN $y = NL$
Rule 4: IF $x_1 = PS$ and $x_2 = NL$ THEN $y = NL$
Rule 5: IF $x_1 = PL$ and $x_2 = NL$ THEN $y = ZE$

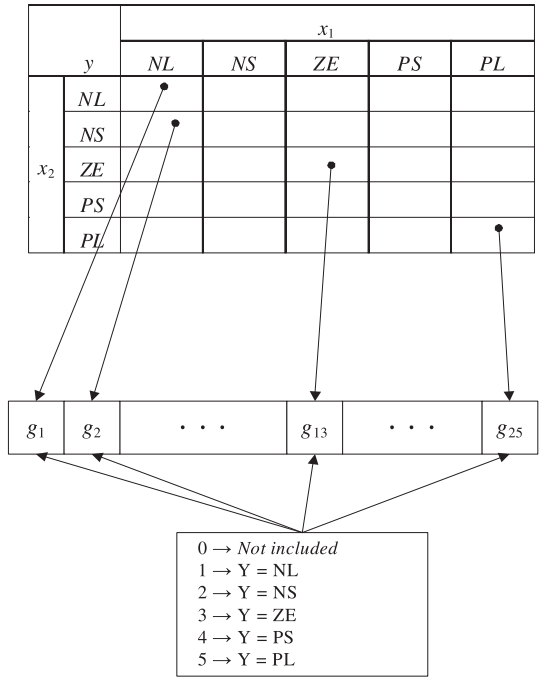

Figure 1. Encoding method for logic rules (Chiou and Lan 2005).

2.1.2. *Encoding method for membership function*

Consider a triangle fuzzy number and let parameters c_k^r, c_k^c, and c_k^l, respectively represent the coordinates of right anchor, cortex, and left anchor of kth linguistic degree. Then 15 parameters need to be calibrated for a variable with five linguistic degrees. Furthermore, it is assumed that the first and last degrees of fuzzy numbers are left- and right-skewed triangles, respectively, and that the others are isosceles triangles as shown in Figure 2. Therefore, a variable with five linguistic degrees has eight parameters to be calibrated and their orders are

$$c_{max} = c_5^c = c_5^r \geqslant c_4^r \geqslant \begin{matrix} c_5^l \\ c_3^r \end{matrix} \geqslant \begin{matrix} c_4^l \\ c_2^r \end{matrix} \geqslant \begin{matrix} c_3^l \\ c_1^r \end{matrix} \geqslant c_2^l \geqslant c_1^c = c_1^l = c_{min}, \quad (1)$$

$$c_k^c = \frac{(c_k^r + c_k^l)}{2}, \quad k = 2, 3, 4, \quad (2)$$

where $c_{\max}$ and $c_{\min}$ are the maximum and minimum values of the variable, respectively. The orders between c_5^l and c_3^r, c_4^l and c_2^r and, c_3^l and c_1^r are indeterminate. In order to tune these eight parameters, nine position variables r_1,…, r_9 are designed as follows:

$$c_2^l = c_{min} + r_1 \times \theta, \quad (3)$$

$$c_1^r = c_2^l + r_2 \times \theta, \quad (4)$$

$$c_3^l = c_2^l + r_3 \times \theta, \quad (5)$$

$$c_2^r = \max\{c_1^r, c_3^l\} + r_4 \times \theta, \quad (6)$$

$$c_4^l = \max\{c_1^r, c_3^l\} + r_5 \times \theta, \quad (7)$$

$$c_3^r = \max\{c_2^r, c_4^l\} + r_6 \times \theta, \quad (8)$$

$$c_5^l = \max\{c_2^r, c_4^l\} + r_7 \times \theta, \quad (9)$$

$$c_4^r = \max\{c_3^r, c_5^l\} + r_8 \times \theta, \quad (10)$$

where $\theta = \frac{(c_{max} - c_{min})}{\sum_{i=1}^{9} r_i}$.

To achieve two significant digits, each position variable is represented by four real-coding genes also depicted in Figure 2. The maximum value of the position variables is 99.99 and the minimum value is 0. Thus, in the example of two state variables and one control variable (each with five linguistic degrees), the chromosome is composed of 108 genes.

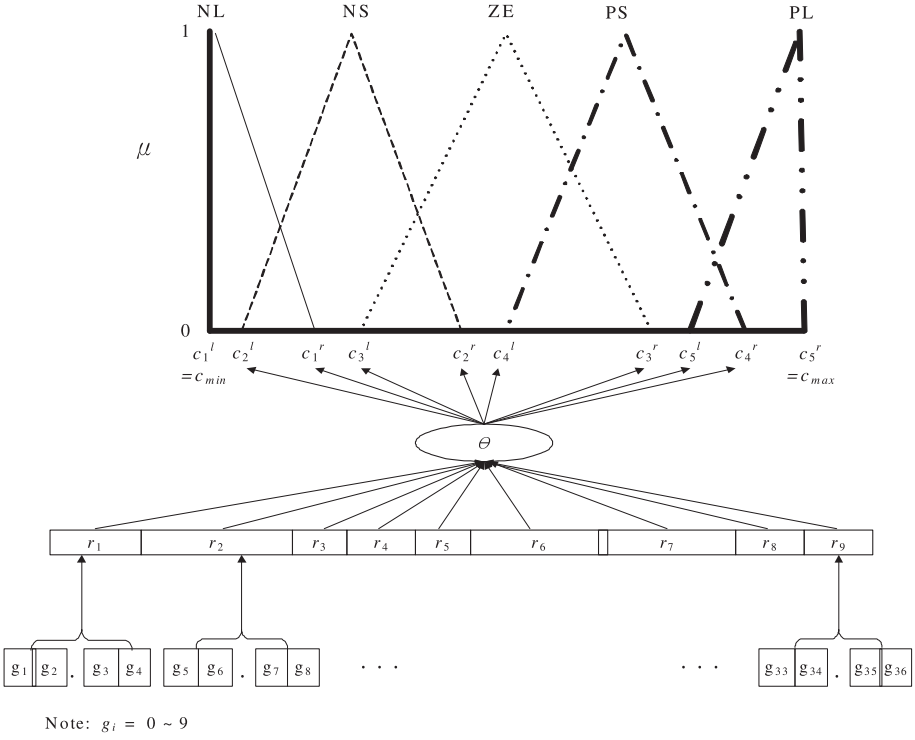

Figure 2. Encoding method for membership functions (Chiou and Lan 2005).

2.1.3. *Genetic operators*

The max-min-arithmetical crossover proposed by Herrera, Lozano, and Verdegay (1995), and the nonuniform mutation proposed by Michalewicz (1992) are employed. In the max-min-arithmetical crossover, let $G_{\mathrm{w}}^t = \{g_{\mathrm{w}1}^t, \ldots, g_{\mathrm{w}k}^t, \ldots, g_{\mathrm{w}K}^t\}$ and $G_{\mathrm{v}}^t = \{g_{\mathrm{v}1}^t, \ldots, g_{\mathrm{v}k}^t, \ldots, g_{\mathrm{v}K}^t\}$ be two chromosomes selected for crossover, the following four offsprings will be generated (Herrera, Lozano, and Verdegay 1995):

$$G_1^{t+1} = aG_w^t + (1-a)G_v^t, \tag{11}$$

$$G_2^{t+1} = aG_v^t + (1-a)G_w^t, \tag{12}$$

$$G_3^{t+1} \text{ with } g_{3k}^{t+1} = \min\{g_{wk}^t, g_{vk}^t\}, \tag{13}$$

$$G_4^{t+1} \text{ with } g_{4k}^{t+1} = \max\{g_{wk}^t, g_{vk}^t\}, \tag{14}$$

where a is a parameter ($0 < a < 1$) and t is the number of generations. In the nonuniform mutation, let $G_j^t = \{g_{j1}^t, \ldots, g_{jk}^t, \ldots, g_{jK}^t\}$ be a chromosome and the gene g_{jk}^t be selected for mutation (the domain of g_{jk}^t is $[g_{jk}^l, g_{jk}^u]$), the value of g_k^{t+1} after mutation can be computed as follows,

$$g_{jk}^{t+1} = \begin{cases} g_{jk}^t + \Delta(t, g_{jk}^u - g_{jk}^t) & \text{if } b = 0, \\ g_{jk}^t - \Delta(t, g_{jk}^t - g_{jk}^l) & \text{if } b = 1, \end{cases} \tag{15}$$

where b randomly takes a binary value of 0 or 1. The function $\Delta(t, z)$ returns a value in the range of [0, z] such that the probability of $\Delta(t, z)$ approaches 0 as t increases:

$$\Delta(t, z) = z(1 - r^{(1-t/T)^h}), \tag{16}$$

where r is a random number in the interval [0, 1], T is the maximum number of generations, and h is a given constant. In Equation (16), the value returned by $\Delta(t, z)$ will gradually decrease as the evolution progresses.

2.1.4. *Iterative evolution algorithm*

The iterative evolution algorithm for selecting the logic rules and tuning the membership functions is similar to bi-level mathematical programming. The upper level is to solve the composition of logic rules using the membership functions tuned by the lower level. The lower level is to determine the shape of membership functions using the logic rules learned from the upper level. Consider an FLC with n state variables $x_1, x_2, \ldots, x_n$ and one control variable y, each with $d_1, d_2, \ldots, d_n$ and d_{n+1} linguistic degrees. Assume the membership functions of all linguistic degrees to be triangle-shaped. The iterative evolution algorithm is structured as follows:

Step 0: Initialization: $s = 1$.
Step 1: Selecting logic rules.
  Step 1–1: Generating an initial population with p chromosomes. Each chromosome has $\prod_{i=1}^{n} d_i$genes, and each gene randomly takes one integer from [0, d_{n+1}].
  Step 1–2: Calculating the fitness values of all chromosomes based on incumbent shapes of membership functions.
  Step 1–3: Selection.
  Step 1–4: Crossover.
  Step 1–5: Mutation.
  Step 1–6: Testing the stop condition. The stop condition is set based on whether the mature rate (the proportion of same chromosome in a population) has reached a given constant η. If so, proceed to Step 2; otherwise go to Step 1–3.
Step 2: Tuning membership functions.
  Step 2–1: Generating an initial population with p chromosomes. Each chromosome has $36(n+1)$ genes and each gene randomly takes one integer from [0, 9].
  Step 2–2: Calculating the fitness values of all chromosomes based on the incumbent combination of logic rules.
  Step 2–3: Selection.
  Step 2–4: Crossover.
  Step 2–5: Mutation.
  Step 2–6: Testing the stop condition. Let f_s be the largest fitness among the population for the *sth* evolution epoch. The stop condition is set based on whether the mature rate has reached a given constant η. If so, proceed to Step 3 and let $s = s + 1$; otherwise go to Step 2–3.
Step 3: Testing the stop condition. If $(f_{s+1} - f_s) \leqq \varepsilon$, where ε is an arbitrary small number, then stop. Incumbent combination of logic rules and shapes of membership functions are the optimal learning results. Otherwise, go to Step 1.

2.2. *The signal control*

2.2.1. *Fitness value*

The performance of signal control for an isolated intersection or sequential intersections is frequently measured in terms of total number of stopped vehicles, proportion of stopped vehicles, average vehicle delays, total vehicle delays (TVD), maximal green band, etc. This study will aim to minimize the TVD and thus defines the fitness function of GAs as follows,

$$f = \frac{1}{TVD}. \tag{17}$$

2.2.2. *Variables*

Following most of the previous literature, this study chooses average traffic flows in green phase (*TF*) and queue length in red phase (*QL*) as two state variables.

The control variable is extension of green time (*EGT*), to determine the timing of phase change. For the case of sequential intersections, *TF* is the summation of traffic flows at all approaches in green phase; while *QL* is the summation of queue length at all approaches in red phase. Assume that these variables are five linguistic degrees and represented by triangle membership functions. This makes a total of 125 potential logic rules. With one gene for each rule, there would be 25 genes in a chromosome; thus, a total of 36 position parameters are required to calibrate the tuning of membership functions. With four genes for each parameter, there would be a total of 108 genes in a chromosome.

2.2.3. *Activation points*

In consideration of pedestrian safe crossing, a minimum green time (G_{min}) in each green phase is preset. At the end of G_{min}, the proposed iterative GFLC model will be activated automatically to conclude an *EGT*. If $EGT \geqslant EGT_{min}$ (a preset value), current green phase will be extended by *EGT* seconds. If $EGT < EGT_{min}$, current green phase will be terminated. The GFLC model will not be activated again until the end of this extension time. If total green time exceeds the preset maximum green time (G_{max}), current green phase is forced to terminate. A short all-red period is designed in each signal change interval. The activation points are also depicted in Figure 3.

2.2.4. *Models comparison*

For validation, the proposed GFLC model is compared with three pretimed plans – Optimal single, Optimal multiple, and Webster, as well as two adaptive timing plans – Vanished queue length (VQL) and Maximum queue length (MQL). The Optimal single timing plan is determined by total enumeration method to search for an optimal cycle length and green time during the study period. The Optimal multiple timing plans comprise some optimal single timing plans which depend on traffic flow patterns. The determination of cycle length and green time of Webster timing plan can be referred to Equations (18–20) and any textbook in traffic control (May 1990; McShane and Roess 1990).

$$C = \frac{1.5L + 5}{1 - y_1 - y_2 - \ldots y_n} = \frac{1.5L + 5}{1 - Y}, \tag{18}$$

where C: cycle length; L: total lost time; y_i: the ratio of maximum flow rate and saturation flow rate in phase i; $Y = \sum y_i$.

$$G_E = C - L, \tag{19}$$

$$G_{Ei} = \frac{y_i}{Y} G_E, \tag{20}$$

where G_E: effective green time; G_{Ei}: green split in phase i.

The VQL based model adopted in Lin and Lo (2008) is an adaptive control system. It switches traffic signal to serve the other approach, whenever the queue on the current approach vanishes. In contrast, the MQL-based model turns the traffic signal into green, whenever the queue length of the approach reaches a preset maximum value which is optimized through trial and error. The activation points of VQL and MQL are depicted in Figures 4 and 5.

2.3. *The CTM*

Previous studies have often employed traffic simulation software to evaluate the performance of signal control models. However, it would be too time-consuming to use simulation software for the evolution of genetic generations. To facilitate the learning process of the proposed model, an efficient traffic simulator is necessary to evaluate the performance of selected logic rules and

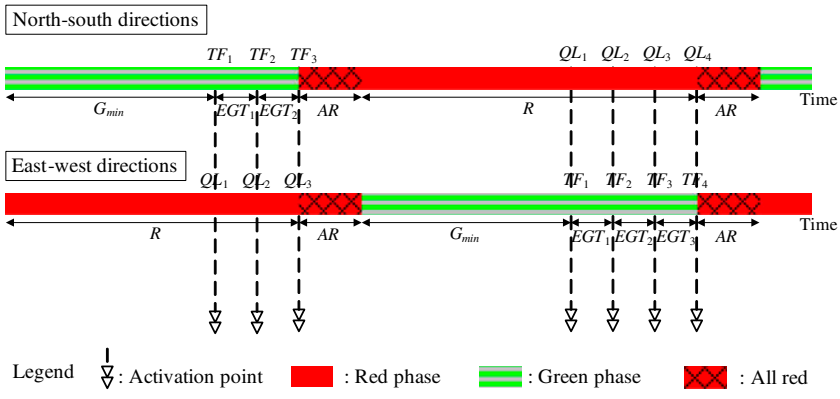

Figure 3. GFLC activation points for an isolated intersection.

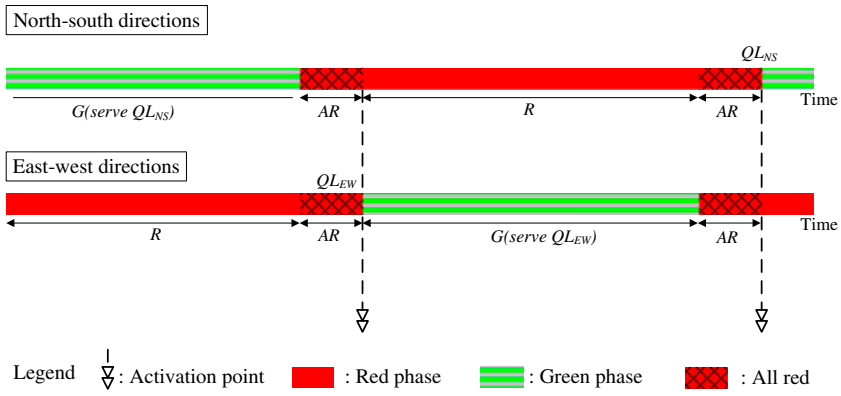

Figure 4. VQL activation points for an isolated intersection.

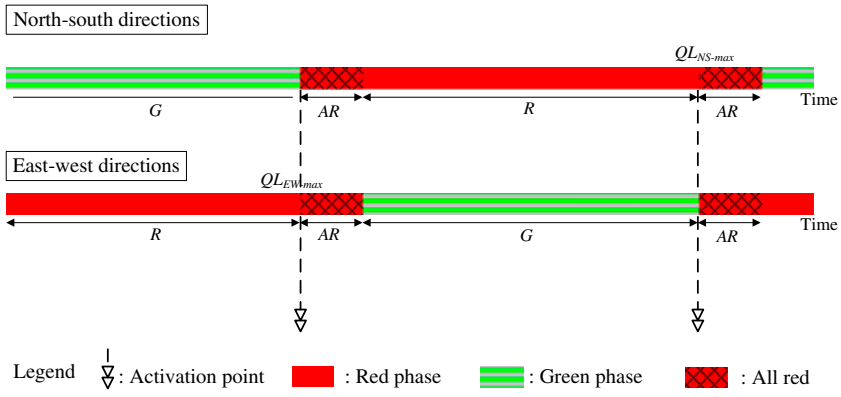

Figure 5. MQL activation points for an isolated intersection.

tuned membership functions in a short period. Thus, a cell-based traffic simulator is considered. CTM, proposed by Daganzo (1994, 1995) for simulating traffic hydrodynamic behavior in a cell-based manner, uses several simple equations to govern traffic movements along the roadway which is represented by a series of equal-length cells. These equations are expressed as follows depending on normal connection, diverging connection, or merging connection (as shown in Figure 6):

2.3.1. *Normal connection*

$$S_{Bk}(t) = \min\{Q_{Bk}(t), n_{Bk}(t)\}, \tag{21}$$

$$R_{Ek}(t) = \min\{Q_{Ek}(t), (w/v_f)(N_{Ek}(t) - n_{Ek}(t))\}, \tag{22}$$

$$q_{Ek}(t) = \min\{S_{Bk}(t), R_{Ek}(t)\}, \tag{23}$$

$$n_{Bk}(t+1) = n_{Bk}(t) - q_{Ek}(t) + q_{jk}(t), \tag{24}$$

$$n_{Ck}(t+1) = n_{Ck}(t) + q_{Ek}(t) - q_{lk}(t), \tag{25}$$

where $S_{Bk}(t)$ represents the potential moving vehicles in cell Bk at time t. $Q_{Bk}(t)$ represents the maximum number of vehicles entering into cell Bk at time t. $n_{Bk}(t)$ represents the number of vehicles in cell Bk at time t. R_{Ek}(t) represents the potential vehicles moving into cell Ek at time t. $N_{Ek}(t)$ represents the maximum number of vehicles stored in cell Ek at time t. v and w are the free-flow and shock-wave speeds, respectively. $q_{Ek}(t)$ represents the number of vehicles flowing into cell Ek from cell Bk at time t. The $q-k$ fundamental diagram can be depicted as Figure 7.

2.3.2. *Diverge connection*

In deriving boundary conditions for divergences, it should be recognized that the left- and right-turning ratios generally depend on the mix of vehicle destinations presenting in cells upstream of the junction. Thus, the cell transmission equations can be expressed as follows:

$$S_{Bk}(t) = \min\{Q_{Bk}(t), n_{Bk}(t)\}, \tag{26}$$

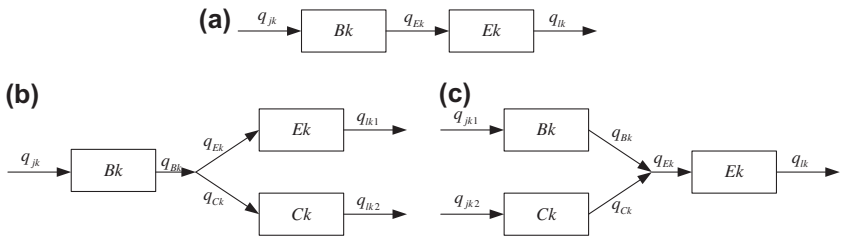

Figure 6. Representation of three connections of CTM. (a) normal, (b) diverge, and (c) merge.

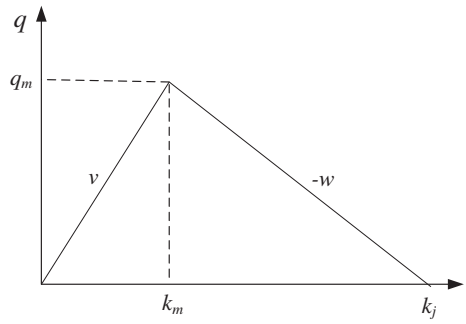

Figure 7. *q-k* diagrams obtained from the CTM.

$$R_{Ek}(t) = \min\{Q_{Ek}(t), (w/v_f)(N_{Ek}(t) - n_{Ek}(t))\}, \quad (27)$$

$$R_{Ck}(t) = \min\{Q_{Ck}(t), (w/v_f)(N_{Ck}(t) - n_{Ek}(t))\}, \quad (28)$$

$$q_{Bk}(t) = \min\{S_{Bk}, R_{Ek}/\beta_{Ek}, R_{Ck}/\beta_{Ck}\}, \quad (29)$$

$$q_{Ek}(t) = \beta_{Ek} q_{Bk}, \quad (30)$$

$$q_{Ck}(t) = \beta_{Ck} q_{Bk}, \quad (31)$$

$$n_{Bk}(t+1) = n_{Bk}(t) - q_{Bk}(t) + q_{jk}(t), \quad (32)$$

$$n_{Ek}(t+1) = n_{Ek}(t) + q_{Ek}(t) - q_{lk1}(t), \quad (33)$$

$$n_{Ck}(t+1) = n_{Ck}(t) + q_{Ck}(t) - q_{lk1}(t), \quad (34)$$

where β_{Ek} and β_{Ck} are left- and right-turning ratios, respectively.

2.3.3. *Merge connection*

A merge can present in one of three following cases:

Case 1: Receiving is more than sending ($R_{Ek} \geqslant S_{Bk} + S_{Ck}$)

$$S_{Bk}(t) = \min\{Q_{Bk}(t), n_{Bk}(t)\}, \quad (35)$$

$$S_{Ck}(t) = \min\{Q_{Ck}(t), n_{Ck}(t)\}, \quad (36)$$

$$R_{Ek}(t) = \min\{Q_{Ek}(t), (w/v_f)(N_{Ek}(t) - n_{Ek}(t))\}, \quad (37)$$

$$q_{Bk}(t) = S_{Bk}, \quad (38)$$

$$q_{Ck}(t) = S_{Ck}, \quad (39)$$

$$q_{Ek}(t) = R_{Ek}, \quad (40)$$

$$n_{Bk}(t+1) = n_{Bk}(t) - q_{Bk}(t) + q_{jk1}(t), \quad (41)$$

$$n_{Ck}(t+1) = n_{Ck}(t) - q_{Ck}(t) + q_{jk2}(t), \quad (42)$$

$$n_{Ek}(t+1) = n_{Ek}(t) + q_{Ek}(t) - q_{lk}(t), \quad (43)$$

Case 2: Receiving is less than sending ($S_{Bk} > R_{Ek}p_k \wedge S_{Ck} > R_{Ek}p_{Ck}$)

If the condition in Case 1 is not satisfied, the model assumes that the maximum number of vehicles, $R_{Ek}(t)$, advance into cell Ek. As long as the supply of vehicles from both approach $S_{Bk}(t)$ and $S_{Ck}(t)$, is not exhausted, assume that a fraction (p_{Ek}) of vehicles comes from cell *Bk* and the remainder (p_{Ck}) from cell *Ck*, where $p_{EK} + p_{CK} = 1$. Thus, Equations (38) and (39) can be modified as follows:

$$q_{Ek}(t) = p_{Ek} R_{Ek}, \quad (44)$$

$$q_{Ck}(t) = p_{Ck} R_{Ek}, \quad (45)$$

Case 3: Sending of one of two cells is limited by receiving

Which is less common, arises when an approach with priority crowds out traffic on its complementary approach. Thus, Case 3 can be expressed by the following two conditions:

(1) $S_{Bk} < R_{Ek}p_k \wedge S_{Ck} > R_{Ek}p_{Ck}$, Equations (38) and (39) can be modified as

$$q_{Bk}(t) = S_{Bk}, \tag{46}$$

$$q_{Ck}(t) = R_{Ek} - S_{Bk}, \tag{47}$$

(2) $S_{Bk} > R_{Ek}p_k \wedge S_{Ck} < R_{Ek}p_{Ck}$, Equations (38) and (39) can be modified as

$$q_{Bk}(t) = R_{Ek} - S_{Ck}, \tag{48}$$

$$q_{Ck}(t) = S_{Ck}, \tag{49}$$

For the cases of isolated and sequential intersections, *TF* is the average traffic flows at all green-phase approaches. While *QL* is the summation of queue length at all red-phase approaches. Vehicle delay at each time tick can be calculated by multiplying queue length (*QL*) at all red-phase approaches with the time tick. The *TVD* is then calculated by summing up the vehicle delay within the whole evaluation horizon.

3. Isolated intersection

To investigate the applicability and performance of the proposed signal control model, comparisons to other signal control models, including Webster, Optimal single, Optimal multiple, and two queue-length based models, are conducted in experiments.

3.1. *An experimental case*

3.1.1. *Data*

To validate the effectiveness and robustness of the proposed iterative GFLC signal control model, an experimental example for an isolated four-leg intersection (Figure 8) is demonstrated. To simplify the analysis, the study neglects the turning traffic. The parameters of the CTM model are set as: free-flow speed = 50 km/h, time step = 2 s, k_j = 130 veh/km/lane. Assume that the intersection has two lanes ($N_i(t)$ = 3.6 veh/cell for all i and t) in each approach with saturation flow of 1800 pcu/hr/lane ($q_{mi}(t)$ = 2.00veh/time step for all i and t). The flow patterns of five-minute flow rates in different approaches are given in Figure 9. A noticeable peak and off-peak traffic patterns are assumed in east and west directions; while rather flat traffic patterns are assumed in north and south directions. The parameters of the iterative GFLC model are set as the same as population size = 100, crossover rate = 0.9, a = 0.3, h = 0.5, η = 80%, ε = 0.05. The center of gravity method is employed for defuzzification. The parameters of signal control are: G_{max} = 100 s, G_{min} = 20 s, all red + lost time = 6 s, EGT_{max} = 20 s, and EGT_{min} = 4 s. Left- and right-turning ratios are both set as 20%.

3.1.2. *Model training*

The training results of the iterative GFLC signal control model for various mutation rates are reported in Table 1.

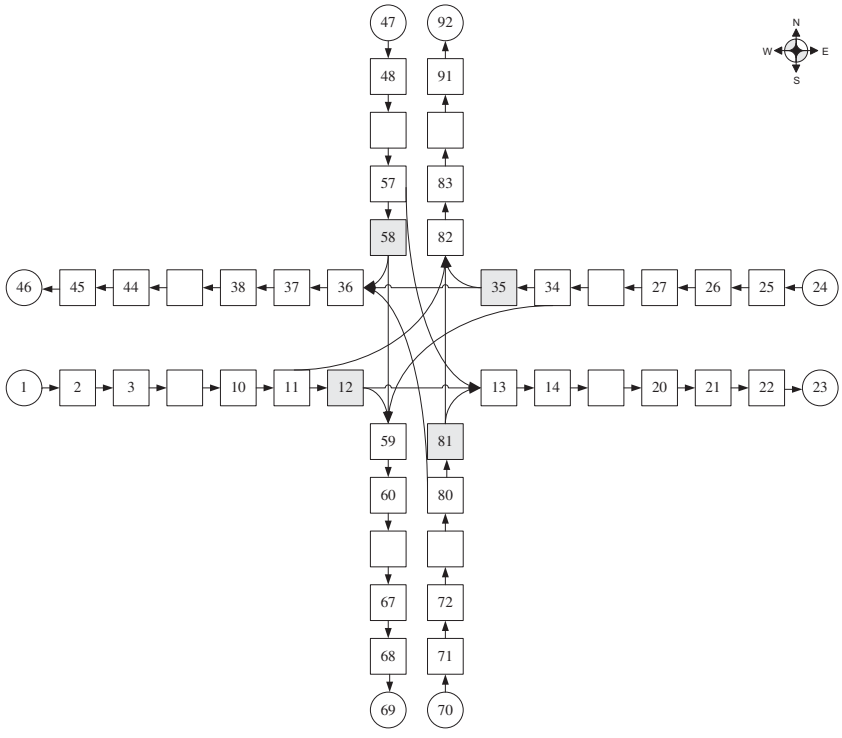

Figure 8. Configuration of the experimental isolated intersection.

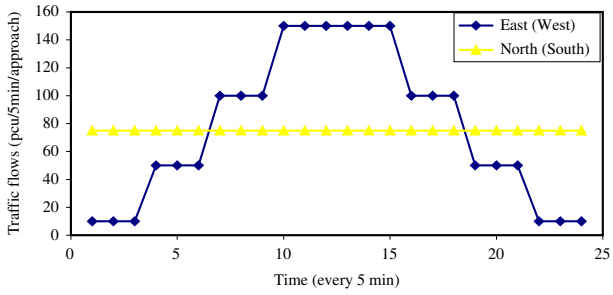

Figure 9. Five-minute flow rates at the experimental isolated intersection.

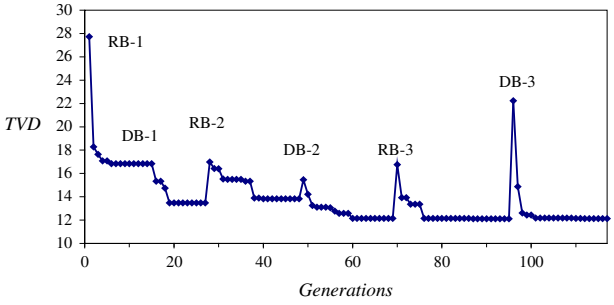

Note: RB-# represents the #th evolution of selecting logic rules. DB-# represents the #th evolution of tuning membership functions.

Figure 10. Learning process of iterative GFLC at the isolated experimental intersection.

As shown in Table 1, the GFLC performs best at the mutation rate of 0.05 with corresponding TVD of 12.13. The values of TVD achieved by the GFLC model under various mutation rates do not significantly differ, but the number of generations tends to rapidly grow as the mutation rate increases. Figure 10 further depicts the learning process of the GFLC at the mutation rate of 0.05. Note that the GFLC converges after three iterative evolutions with 117 generations. The value of *TVD* decreases from 27.73 to 12.31.

Table 2 presents the selected logic rules and Figure 11 shows the tuned membership functions for traffic flow, queue length, and EGT by GFLC. Note from Table 1 that seven and five out of fifteen logic rules have concluded that EGT are '*NL*' and '*NS*', and two and only one logic rule has concluded that *EGT* are '*ZE*' and '*PS*'. Thus, those fifteen logic rules being selected were represented as follows:

Note also from Figure 11(c) that the membership function of '*NL*' degree ranging from 0 to 9 s implies that the rules of concluding '*NL*' tend to terminate the current green phase if EGT is less than 4 s or to extend the green phase if EGT is between 4 and 9 s. The membership functions of '*NS*', '*ZE*', and '*PS*', respectively ranging from 5 to 10, 9 to 13 and 10 to 18 s suggest that the rule of concluding '*NS*', '*ZE*', and '*PS*' tends to extend the current green phase.

3.1.3. *Model validation and comparisons*

To validate the effectiveness, the control performance of iterative GFLC model is compared with three pretimed plans – Optimal single, Optimal multiple, Webster, and two adaptive timing plans – VQL and MQL. The Optimal single timing plan is determined by total enumeration method to search for an optimal cycle length and green time during the study period. The Optimal multiple timing plan comprises eight optimal single timing plans which depend on traffic flow patterns as shown in Figure 9. Since the Optimal multiple model designs the optimal signal timings for each traffic flow rate, its control performance is optimal if traffic pattern remains unchanged. The determination of cycle length and green time for Webster timing plan can be referred to Equations (18–20). The VQL based model adopted in Lin and Lo (2008) is an adaptive control system switching traffic signals to serve the other approach, whenever the queue on the current approach vanishes. In contrast, the MQL based model turns traffic signal green whenever the queue length of the approach reaches a preset maximum value which is optimized through a trial and error.

Table 3 summarizes the comparison results. The Optimal multiple timing plan, composed of eight optimal single timing plans, each of which lasts for 15 min, corresponding to various traffic conditions, is the optimal control under the given traffic conditions. Notice that only 0.13 vehicle-hours or 1.08% additional delays are incurred by iterative GFLC model in comparison with the optimal multiple timing plan. In other words, the GFLC model has achieved almost optimal control. Also notice that the GFLC model performs better than Webster, Optimal single, VQL, and MQL models by respectively curtailing 6.47, 4.40, 1.88, and 1.36 vehicle-hours (or 34.78, 26.62, 13.42, and 10.08%) of TVD. The results demonstrate the effectiveness of our proposed iterative GFLC model. The performance comparison between the Optimal multiple timing plan and the proposed GFLC model shows that our proposed GFLC model can achieve almost optimal control.

Table 1. The results of iterative GFLC with various mutation rates (Pm).

Pm	0.01	0.03	0.05	0.07	0.10	0.20	0.30	0.40	0.50
No. of generations	233	173	117	319	195	365	262	1054	1331
TVD	12.35	12.25	12.13	12.41	12.89	12.91	12.61	12.30	12.20

Table 2. Selected logic rules by iterative GFLC.

Y (EGT)		X_1 (TF)				
		NL	NS	ZE	PS	PL
X_2 (QL)	NL	NS	ZE	NS		
	NS	NL	ZE	NS		
	ZE	ZE	NS	NL		
	PS	NS	PS	NS	NS	PS
	PL	NS	PL	PS	PS	NL

Rule 1: IF $TF = NL$ and $QL = NL$ THEN $EGT = NS$.
Rule 2: IF $TF = NL$ and $QL = NS$ THEN $EGT = NL$.
Rule 3: IF $TF = NL$ and $QL = ZE$ THEN $EGT = ZE$.
Rule 4: IF $TF = NL$ and $QL = PS$ THEN $EGT = NS$.
Rule 5: IF $TF = NL$ and $QL = PL$ THEN $EGT = NS$.
Rule 6: IF $TF = NS$ and $QL = NL$ THEN $EGT = ZE$.
Rule 7: IF $TF = NS$ and $QL = NS$ THEN $EGT = ZE$.
Rule 8: IF $TF = NS$ and $QL = ZE$ THEN $EGT = NS$.
Rule 9: IF $TF = NS$ and $QL = PS$ THEN $EGT = PS$.
Rule 10: IF $TF = NS$ and $QL = PL$ THEN $EGT = PL$.
Rule 11: IF $TF = ZE$ and $QL = NL$ THEN $EGT = NS$.
Rule 12: IF $TF = ZE$ and $QL = NS$ THEN $EGT = NS$.
Rule 13: IF $TF = ZE$ and $QL = ZE$ THEN $EGT = NL$.
Rule 14: IF $TF = ZE$ and $QL = PS$ THEN $EGT = NS$.
Rule 15: IF $TF = ZE$ and $QL = PL$ THEN $EGT = PS$.
Rule 16: IF $TF = PS$ and $QL = PS$ THEN $EGT = NS$.
Rule 17: IF $TF = PS$ and $QL = PL$ THEN $EGT = PS$.
Rule 18: IF $TF = PL$ and $QL = PS$ THEN $EGT = PS$.
Rule 19: IF $TF = PL$ and $QL = PL$ THEN $EGT = NL$.

The eastwest cycle length and green splits in each cycle by GFLC are illustrated in Figure 12and in which a total of 102 cycles are progressed with cycle lengths ranging from 56 to 110 s. The distribution of northsouth green splits in Figure 12(b) has approximately reflected the traffic patterns of the same directions in Figure 9. This indicates that our iterative GFLC model can control the traffic signal adaptively.

To further examine the robustness of the iterative GFLC model, we randomly vary the traffic flows by 10–50% as shown in Figure 13. The timing plans of pretimed signal control models (i.e. Webster, Optimal single, and Optimal multiple) remain unchanged. The GFLC timing plans corresponding to various traffic flows are generated by the same logic rules and membership functions, which are learned from the original traffic patterns as given in Subsection 3.1.2. The results are summarized in Table 4. Note that the GFLC outperforms the three pretimed and two adaptive control timing plans. Moreover, the GFLC can do much better than any other models as the traffic flows vary more conspicuously, indicating the robustness of the GFLC model.

Table 3. Comparison of control performance at the experimental isolated intersection.

Timing plan	*TVD* (vehicle-hours)	*ΔTVD* compared with GFLC	
		Vehicle-hours	%
GFLC	12.13	–	–
Webster	18.60	6.47	34.78
Optimal single	16.53	4.40	26.62
Optimal multiple (8)	12.00	−0.13	−1.08
MQL	14.01	1.88	13.42
VQL	13.49	1.36	10.08

Note: Optimal multiple (8) represents a total of sub-periods. The *TVD* of each sub-period is determined by the optimal single timing plan.

The sensitivity analysis of different percentages of turning flow is shown in Table 5. The timing plans of all models also remain unchanged. Note that the GFLC has outperformed other timing plans at each level of turning flow rates, except the training case ($P_{LT} = 0.2$, $P_{RT} = 0.2$). Moreover, the GFLC can do much better than any other models as the turning flows increase.

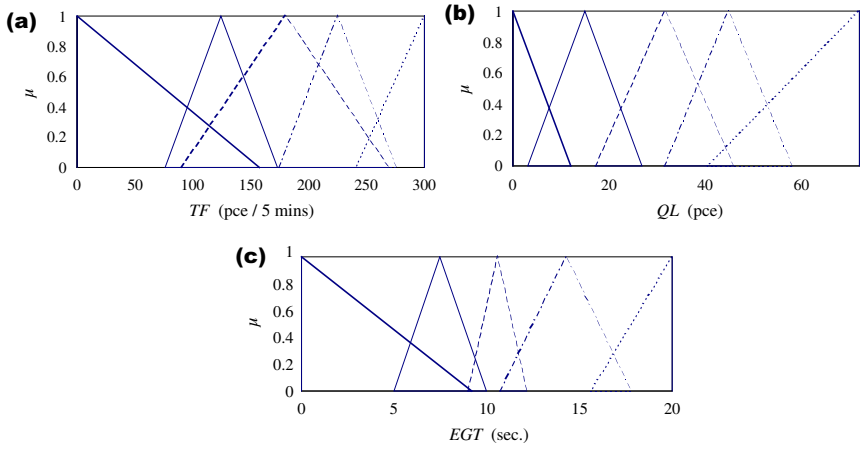

Figure 11. Tuned membership functions by iterative GFLC. (a) traffic flow (TF), (b) queue length (QL), and (c) extension of green time (EGT).

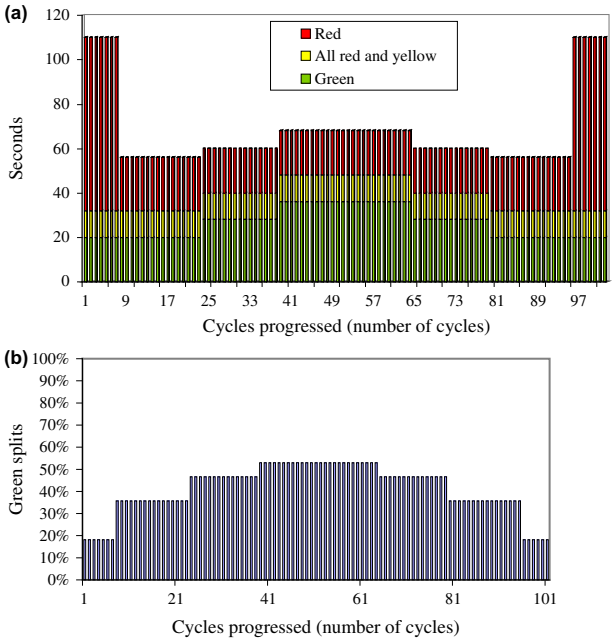

Figure 12. Eastwest cycle length and green splits by the GFLC at the experimental isolated intersection. (a) Cycle length, (b) Green splits.

4. Coordinated intersections

This study further extends the proposed iterative GFLC model to the signal control of consecutive intersections. To synchronize the signal control for sequential intersections, three coordinated signal systems including simultaneous, alternate, and progressive systems are considered. The simultaneous system implements exactly the same signal timing plans simultaneously in sequential intersections without offset (time lag). The progressive system implements these plans with offset. The alternative system implements two timing plans with inverse green and red times. In addition, an independent operation which implements the timing plans at the sequential intersections without any coordination is also compared. The timing plans of these four signal systems are determined by the GFLC model and Optimal multiple model, respectively. In other words, a total of eight timing plans are to be generated and compared.

4.1. *An experimental case*

4.1.1. *Data*

An experimental example with two consecutive four-leg intersections (Figure 14) is demonstrated. Assume that the intersections have two lanes in each approach with saturation flow of 1800 pcu/hr/lane. The distance between intersections is 222 meters with 8 cells. The five-minute flow rates in different approaches are shown in Figure 15. In this experimental example, a noticeable peak and off-peak traffic patterns are assumed in east and west directions; while rather flat traffic patterns are assumed in north and south directions. The offset of progressive coordinated system is 16 s, since the speed limit between intersections is set as 50 km/hr.

4.1.2. *Model comparisons*

To validate effectiveness, the control performance of GFLC is compared with Optimal multiple pretimed models with two sub-periods. All signal timing plans of GFLC and Optimal multiple models under various coordinated systems are determined separately. To avoid lengthy discussion, the learning results of GFLC are not reported. The control performances of these eight signal control models are reported and compared with Table 6. Obviously, the performances under a progressive coordinated system are significantly superior to other systems. Progressive GFLC is the best among these four models with a total delay of 37.35 vehicle hours, followed by progressive optimal multiple model with a total delay of 42.96 vehicle hours. The signal control models under alternate coordinated system perform relatively poorly. Also notice that all GFLC signal control models perform better than the optimal multiple

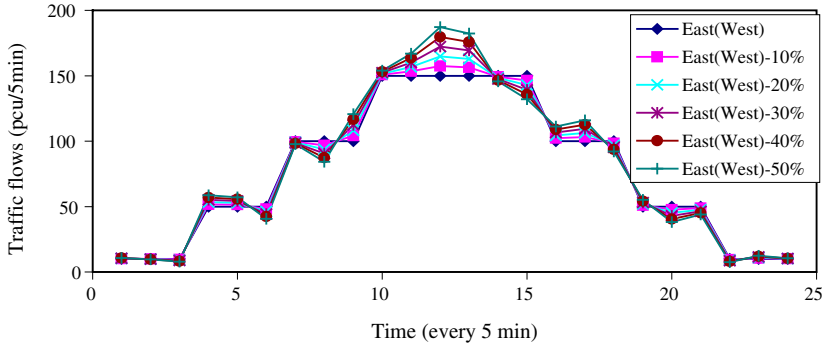

Figure 13. Varied five-minute flow rates at the experimental isolated intersection.

Table 4. Comparison of control performance with randomly varied flow rates.

Timing plan	10%		20%		30%		40%		50%	
	TVD	*ΔTVD %*	*TVD*	*ΔTVD %*	*TVD*	*ΔTVD %*	*TVD*	*ΔTVD %*	*TVD*	*ΔTVD %*
GFLC	12.98	–	13.47	–	14.41	–	15.02	–	15.54	–
Webster	20.14	35.55	20.97	35.77	22.57	36.15	24.54	38.79	26.65	41.68
Optimal single	17.75	26.87	19.03	29.22	21.54	33.10	22.91	34.44	23.78	34.65
Optimal multiple	13.45	3.49	13.98	3.65	15.09	4.51	16.55	9.24	18.12	14.24
MQL	15.32	15.27	15.97	15.65	17.41	17.23	18.31	17.97	19.12	18.72
VQL	14.51	10.54	15.09	10.74	16.21	11.10	16.97	11.49	17.57	11.55

Table 5. Comparison of control performance with increased turning flow rates.

Models	0.2		0.4		0.6	
	TVD	*ΔTVD%*	*TVD*	*ΔTVD%*	*TVD*	*ΔTVD%*
P_{LT} (P_{RT}=0.2 P_S=1 − P_{LT} − P_{RT})						
GFLC	12.13	–	15.32	–	19.32	–
Webster	18.6	34.78	27.98	45.25	36.14	46.54
Optimal single	16.53	26.62	25.24	39.30	33.65	42.59
Optimal multiple	12.00	−1.08	18.07	15.22	23.67	18.38
MQL	14.01	13.42	17.81	13.98	22.6	14.51
VQL	13.49	10.08	18.44	16.92	23.54	17.93
P_{RT} (P_{LT}=0.2 P_S=1 − P_{LT} − P_{RT})						
GFLC	12.13	–	14.99	–	17.90	–
Webster	18.6	34.78	24.64	39.16	30.88	42.03
Optimal single	16.53	26.62	20.85	28.11	25.64	30.19
Optimal multiple	12.00	−1.08	17.19	12.80	21.13	15.29
MQL	14.01	13.42	17.38	13.75	21.09	15.13
VQL	13.49	10.08	17.69	15.26	22.31	19.77

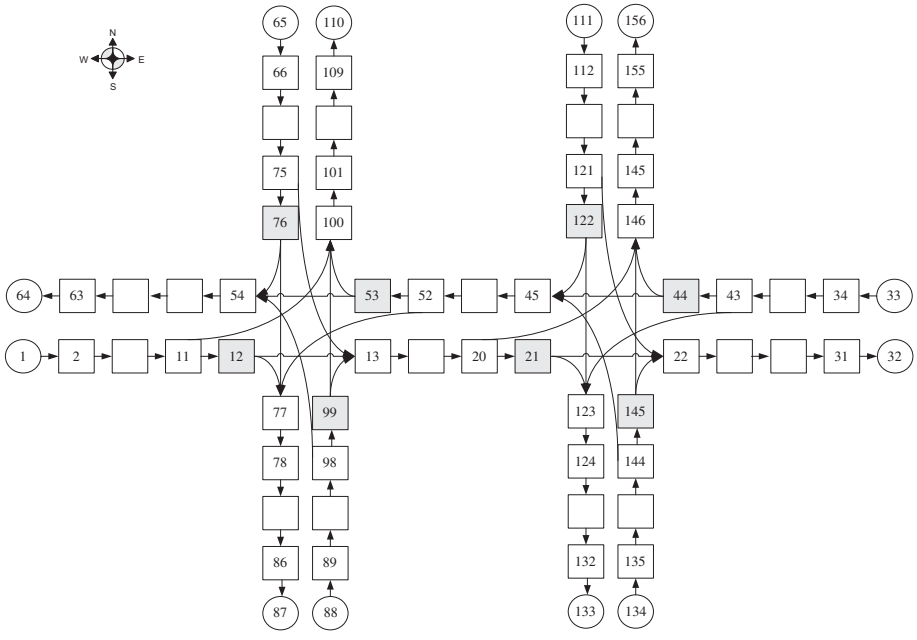

Figure 14. Configuration of the experimental sequential intersections.

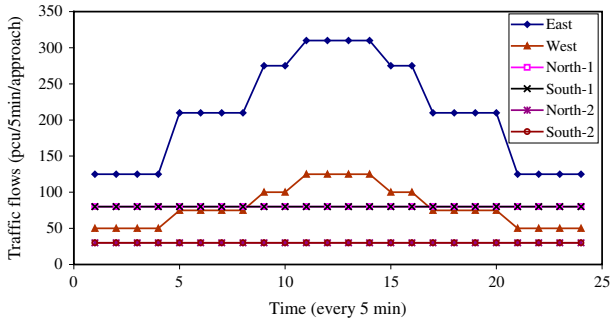

Note: north-# and south-# represent the traffic flows in north and south directions, respectively, at intersection #.

Figure 15. Five-minute flow rates at the experimental sequential intersections.

Table 6. Comparison of control performance at experimental sequential intersections.

Signal coordinated system	*TVD* (vehicle-hours)		Rate of *ΔTVD* reduced by GFLC (%)
	GFLC	Optimal multiple (2)	
Simultaneous	43.23	49.02	11.82
Progressive	37.35	42.96	13.06
Alternate	50.19	55.17	9.02
Independent	46.00	51.38	10.48

models. Compared with the optimal multiple model under the same coordinated system, progressive GFLC can curtail the total delay by the largest amount (13.06%), followed by simultaneous GFLC (11.82%) and by independent GFLC (10.48%). The results show the effectiveness of the proposed iterative GFLC models in controlling sequential intersections.

Six scenario analyses, varying the flow rates in east-west directions and holding the northsouth flows unchanged were conducted. Three levels of flow rates are assumed: the eastbound flow rate is considered as the high level, the westbound flow rate is the low level, and the average of the eastbound and westbound flow rate is defined as the medium level. The control performances of these six scenarios are reported in Table 7 and in which Scenario 6 is the original case. Note that in the cases of same traffic flow level in eastwest direction (scenarios 1, 2 and 3), the rates of TVD reduction by GFLC become more significant as the east west traffic flows get higher. Compared with the optimal multiple models, GFLC can curtail TVD by 17.56% in scenario 1 with progressive coordinated system. However, in the cases of different traffic flow levels in eastwest direction (scenarios 4, 5 and 6), noticeable reduction in TVD by GFLC can be found only for scenario 6 with progressive systems (13.06%).

Table 7. Comparison of control performance with varied east west traffic flow scenarios.

Scenarios	Traffic flow		Coordinated system	*TVD* (vehicle-hours)		Rate of *ΔTVD* reduced by GFLC (%)
	Eastbound	Westbound		GFLC	Optimal multiple (2)	
1	High	High	Simultaneous	67.09	81.23	17.40
			Progressive	63.99	77.62	17.56
			Alternate	85.27	100.49	15.15
			Independent	72.47	86.34	16.06
2	Medium	Medium	Simultaneous	42.44	47.84	11.28
			Progressive	32.23	36.68	12.12
			Alternate	51.67	55.69	7.23
			Independent	44.69	47.84	6.59
3	Low	Low	Simultaneous	26.68	28.83	7.44
			Progressive	16.10	17.99	10.48
			Alternate	46.32	49.70	6.80
			Independent	33.83	35.76	5.39
4	High	Medium	Simultaneous	58.54	62.71	6.65
			Progressive	54.84	60.18	8.87
			Alternate	78.37	82.68	5.21
			Independent	68.25	72.13	5.38
5	Medium	Low	Simultaneous	37.38	39.54	5.45
			Progressive	20.86	22.59	7.67
			Alternate	49.52	51.78	4.35
			Independent	36.53	38.34	4.74
6	High	Low	Simultaneous	43.23	49.02	11.82
			Progressive	37.35	42.96	13.06
			Alternate	50.19	55.17	9.02
			Independent	46.00	51.38	10.48

5. Concluding remarks

Based on the iterative GFLC model proposed by Chiou and Lan (2005), this study further develops an adaptive signal control model for both isolated and sequential intersections. We choose average traffic flow and queue length as state variables, EGT as control variable, and TVD as performance measurement. In order to evaluate control performance accurately, the CTM is used to replicate traffic behaviors. For the case of an isolated intersection, the experimental example has shown that the control performance of GFLC is almost the same as the optimal multiple timing plan and superior to the optimal single, Webster, VQL, and MQL-based timing plans. In the case of sequential intersections, the experimental example has also shown that GFLC performs better than the optimal multiple model, no matter which coordinated signal system is operated. These results demonstrate that the proposed GFLC model is effective, robust, and applicable to real-time signal control.

To further improve the control performance, more effective and efficient encoding methods in selecting the logic rules or tuning the membership functions or both deserve to be explored. It would be interesting to examine whether the learning results of GFLC, the composition of logic rules and the shapes of tuned membership functions are interpretable or not. If so, GFLC can explain an expert's judgment or decision; otherwise it just works like a black box. For sequential intersections, the performance is measured by TVD in this study; it can also be replaced by other measurement such as green band or stopping ratio along the arterial. Because of the computational efficiency of the proposed model, applications to a large-scale network deserve further examination. However, it should be noted that the control performance would be greatly degraded as the number of coordinated intersections increases. Thus, to combine with an intersection clustering algorithm, the proposed model is able to not only conduct adaptive signal control but also to determine which intersections have to be coordinated. Last but not least, to better account for traffic behavior on many Asian urban streets, mixed traffic including cars, motorcycles, and buses should be considered in signal control model.

Acknowledgments

The authors are indebted to two anonymous reviewers for their insightful comments and constructive suggestions, which helped clarify several points made in the original manuscript. This study was financially sponsored by the ROC National Science Council (NSC 100-2221-E-009-121).

Nomenclature

NL, NS, ZE, PS, PL	five linguistic degrees
c_{max}	the maximum value of the corresponding variable
c_{min}	the minimum value of the corresponding variable
c_k^r	the coordinate of right anchor of the kth linguistic degree
c_k^c	the coordinate of cortex of the kth linguistic degree
c_k^l	the coordinate of left anchor of the kth linguistic degree
$r_1,\ldots, r_9$	the position parameters
t	number of generations
r	random number
T	the maximum number of generations
G_j^t	the jth chromosome in the tth generation
g_{jk}^t	the kth gene of the jth chromosome in the tth generation
g_{jk}^l	lower bound of g_{jk}^t for all generations
g_{jk}^u	upper bound of g_{jk}^t for all generations
a	a preset parameter ($0 < a < 1$)
b	binary number which randomly takes a value of 0 or 1
f_s	the largest fitness value among the population
TVD	total vehicle delays
TF	average traffic flows in green phase
QL	queue length in red phase
EGT	extension of green time
G_{min}	minimum green time
EGT_{max}	the maximum value of EGT
EGT_{min}	the minimum value of EGT
C	cycle length
L	total lost time
y_i	the ratio of maximum flow rate and saturation flow rate in phase
G_E	effective green time
G_{Ei}	green split in phase i
$S_{Bk}(t)$	the potential moving vehicles in cell Bk at time t
$Q_{Bk}(t)$	the maximum number of vehicles entering into cell Bk at time t
$n_{Bk}(t)$	the number of vehicles in cell Bk at time t
$R_{Ek}(t)$	the potential vehicles moving into cell Ek at time t
$N_{Ek}(t)$	the maximum number of vehicles stored in cell Ek at time t
$q_{Ek}(t)$	the number of vehicles flowing into cell Ek from cell Bk at time t
v	free-flow speed
w	shockwave speed
β_{Ek}	left-turning ratio
β_{Ck}	right-turning ratio
p_{Ek}	a fraction of vehicles comes from cell Bk to cell Ek
p_{Ck}	a fraction of vehicles comes from cell Bk to cell Ck

References

Ben-Akiva, M., D. Cuneo, M. Hasan, M. Jha, and Q. Yang. 2003. "Evaluation of Freeway Control using a Microscopic Simulation Laboratory." *Transportation Research Part C* 11 (1): 29–50.

Chiou, Y. C., and L. W. Lan. 2005. "Genetic Fuzzy Logic Controller: An Iterative Evolution Algorithm with New Encoding Method." *Fuzzy Sets and Systems* 152 (3): 617–635.

Chiou, Y. C., Y. F. Huang, and P. C. Lin. 2010. "Optimal Variable Speed-Limit Control under Abnormal Traffic." *Journal of the Chinese Institute of Engineers* 35 (3): 299–308.

Daganzo, C. 1994. "The Cell Transmission Model: A Dynamic Representation of Highway Traffic Consistent with the Hydrodynamic Theory." *Transportation Research Part B* 28 (4): 269–287.

Daganzo, C. 1995. "The Cell Transmission Model, Part II: Network Traffic." *Transportation Research Part B* 29 (2): 79–93.

Dion, F., H. Rakha, and Y. Zhang. 2004. "Evaluation of Potential Transit Signal Priority Benefits along a Fixed-Time Signalized Arterial." *Journal of Transportation Engineering* 130 (3): 294–303.

Fang, F. C., and L. Elefteriadou. 2010. "Modeling and Simulation of Vehicle Projection Arrival–Discharge Process in Adaptive Traffic Signal Controls." *Journal of Advanced Transportation* 44 (3): 176–192.

Herrera, F., M. Lozano, and J. L. Verdegay. 1995. "Tuning Fuzzy Logic Controllers by Genetic Algorithms." *International Journal of Approximate Reasoning* 12 (3–4): 299–315.

Herrera, F., M. Lozano, and J. L. Verdegay. 1998. "A Learning Process for Fuzzy Control Rules using Genetic Algorithms." *Fuzzy Sets and Systems* 100 (1–3): 143–158.

Hoyer, R., and U. Jumar. 1994. "An advanced Fuzzy Controller for Traffic Lights." *Annual Review in Automatic Programming* 19: 67–72.

Lekova, A., L. Mikhailov, D. Boyadjiev, and A. Nabout. 1998. "Redundant Fuzzy Rules Exclusion by Genetic Algorithms." *Fuzzy Sets and Systems* 100 (1–3): 235–243.

Lighthill, M. J., and J. B. Whitham. 1955. "On Kinematic Waves. I. Flow Movement in Long Rivers. II. A Theory of Traffic Flow on Long Crowded Reads." In: *Proceedings of Royal Society* 229 (1178): 281–345. London, UK, 10 May 1955.

Lin, W. H., and D. Ahanotu. 1995. *Validating the Basic Cell Transmission Model on a Single Freeway Link*. Technical note, UCB-ITS-PATH-TN-95-3. Berkeley, CA: University of California.

Lin, L. T., L. W. Tung, and H. C. Ku. 2010. "A Synchronized Signal Control Model for Maximizing Progression along an Arterial." *Journal of Transportation Engineering* 136 (8): 727–735.

Lin, W. H., and H. K. Lo. 2008. "A Robust Quasi-Dynamic Traffic Signal Control Scheme for Queue Management." In *Proceedings of the Thirteenth International Conference of Hong Kong Society for Transportation Studies*, Hong Kong, 13–15 December 2008: 563-572. Hong Kong: HKSTS.

Lo, H. K. 2001. "A Cell-Based Traffic Control Formulation: Strategies and Benefits of Dynamic Timing Plans." *Transportation Science* 35 (2): 148–164.

Lo, H. K., and W. Y. Szeto. 2002. "A Cell-Based Dynamic Traffic Assignment Model: Formulation and Properties." *Mathematical and Computer Modeling* 35 (7–8): 849–865.

May, A. D. 1990. *Traffic Flow Fundamentals*. Englewood Cliffs, NJ: Prentice Hall.

McShane, W. R., and R. P. Roess. 1990. *Traffic Engineering*. Englewood Cliffs, NJ: Prentice Hall.

Michalewicz, Z. 1992. *Genetic Algorithms + Data Structures = Evolution Programs*. Berlin: Springer.

Mohamed, B. T., S. K. Mohamed, and A. Murali. 1999. "A Two-Stage Fuzzy Logic Controller for Traffic Signals." *Transportation Research Part C* 7 (6): 353–367.

Munoz, L., X. Sun, D. Sun, G. Gomes, and R. Horowitz. 2004. Methodological Calibration of the Cell Transmission Model. In *Proceedings of the 2004 American Control Conference* 1 798–803. Boston, MA, June 30–July 2.

Murat, Y. S., and E. Gedizlioglu. 2005. "A Fuzzy Logic Multi-Phased Signal Control Model for Isolated Junctions." *Transportation Research Part C* 13 (1): 19–36.

Niittymäki, J. 2001. "Installation and Experiences of Field Testing a Fuzzy Logic Controller." *European Journal of Operational Research* 131 (2): 273–281.

Pappis, C. P., and E. H. Mamdani. 1977. "A Fuzzy Logic Controller for a Traffic Junction." *IEEE Transactions on Systems, Man and Cybernetics* 7 (10): 707–717.

Pham, V. C., F. Alam, J. Potgieter, F. C. Fang, and W. L. Xu. 2011. "Integrated Fuzzy Signal and Ramp-Metering at a Diamond Interchange." *Journal of Advanced Transportation.* doi: 10.1002/atr.167.

Richard, P. I. 1956. "Shockwaves on the Highway." *Operations Research* 4 (1): 42–51.

Smilowitz, K., and C. Daganzo. 1999. *Predictability of Time-Dependent Traffic Backups and Other Reproducible Traits in Experimental Highway Data*. Working paper UCB-ITS-PWP-99-5, California PATH Program. Berkeley, CA: Institute of Transportation Studies, University of California.

Teodorovic, D. 1999. "Fuzzy Logic Systems for Transportation Engineering: The State of the Art." *Transportation Research Part A* 33 (5): 337–364.

Waller, S., and A. Ziliaskopoulos. 2001. "Stochastic Dynamic Network Design Problem." *Transportation Research Record* 1771 (01–2517): 106–113.

Wang, L., and J. Yen. 1999. "Extracting Fuzzy Rules for System Modeling using a Hybrid of Genetic Algorithms and Kalman Filter." *Fuzzy Sets and Systems* 101 (3): 353–362.

Wong, C. K., S. C. Wong, and H. K. Lo. 2010. "A Spatial Queuing Approach to Optimize Coordinated Signal Settings to Obviate Gridlock in Adjacent Work Zones." *Journal of Advanced Transportation* 44 (4): 231–244.

Wu, Y. Z., and C. H. Ho. 2009. "The Development of Taiwan Arterial Traffic-Adaptive Signal Control System and its Field Test: A Taiwan Experience." *Journal of Advanced Transportation* 43 (4): 455–480.

Xu, H., and M. Zheng. 2009. "Impact of Phase Scheme on Development and Performance of a Logic Rule-Based Bus Rapid Transit Signal Priority." *Journal of Transportation Engineering* 135 (12): 953–965.

Zadeh, L. 1973. "Outline of a New Approach to the Analysis Of Complex Systems and Decision Processes." *IEEE Transactions on Systems, Man and Cybernetics* 3 (1): 28–44.

Zhang, M., S. Ritchie, and W. Recker. 1996. "Some General Results on the Optimal Ramp Control Problem." *Transportation Research Part C* 4 (2): 51–69.